Optics Communications 367 (2016) 155–160

Contents lists available at ScienceDirect

Optics Communications

journal homepage: www.elsevier.com/locate/optcom

Optical pulse compression reflectometry based on single-sideband modulator driven by electrical frequency-modulated pulse

Weiwen Zou [a,b,*], Lei Yu [a], Shuo Yang [a], Jianping Chen [a,b]

[a] State Key Laboratory of Advanced Optical Communication Systems and Networks, Department of Electronic Engineering, Shanghai Jiao Tong University, Shanghai 200240, China

[b] Shanghai Key Lab of Navigation and Location Services, Shanghai Jiao Tong University, Shanghai 200240, China

ARTICLE INFO

Article history:
Received 22 December 2015
Received in revised form
12 January 2016
Accepted 13 January 2016
Available online 4 February 2016

Keywords:
Fiber optics sensors
Frequency modulation
Optical pulse compression reflectometry

ABSTRACT

We propose a novel scheme to generate a linear frequency-modulated optical pulse with high extinction ratio based on an electrical frequency-modulated pulse and optical single-sideband modulator. This scheme is proved to improve the stability and accuracy of optical pulse compression reflectometry (OPCR). In the experiment, a high spatial resolution of 10 cm and a long measurement range of 10.8 km using a laser source with 2-km coherence length are demonstrated.

1. Introduction

Optical fiber reflectometry is an important instrument to monitor intrinsic or external disturbance in optical fibers [1]. Different types of reflectometries have been proposed [2–5]. The first type of optical time domain reflectometry (OTDR) dates back to 1970s [2], which has been widely used for long-length interrogation although its spatial resolution was limited due to the required pulse energy and the intrinsic fiber attenuation. Another reflectometry, called optical frequency domain reflectometry (OFDR) [3], was developed to overcome such shortage since it is referred to the frequency modulation continuous wave (FWCW) radar technology. However, the measurement range of OFDR is physically limited by the half of coherence length of the laser source. In comparison, optical coherence domain reflectometry (OCDR) [4] and optical low coherence reflectometry (OLCR) [5] can also provide competitive spatial resolution but the measurement range is confined as well. Most recently, we proposed a new reflectometry inspired by pulse-compression radar [6], named pulse-compression OTDR [7] or optical pulse compression reflectometry (OPCR) [8], which can overwhelm the tradeoff between the spatial resolution and measurement range. An optical pulse with a long pulse duration and linear frequency modulation (LFM) is launched into an optical fiber and the backscattered light is coherently detected using matched filtering so as to significantly compress the original pulse duration. Consequently, OPCR is able to achieve a high spatial resolution and large signal to noise ratio, both of which are attributed to the wide LFM bandwidth.

In this work, we demonstrate a new-scheme OPCR by use of one optical single-sideband modulator (SSBM) and an electrically pulsed linear frequency modulation. Compared with the previous scheme based on two modulators [8], the new scheme can generate the electric pulsed LFM and optical LFM pulse with less complexity, broader bandwidth and larger extinction ratio. We successfully achieve 10 cm spatial resolution over 10.8 km measurement range although a laser source with coherence length of only 2 km is used.

2. Principle and experimental setup

Fig. 1 compares two schemes generating an optical LFM pulse for the OPCR with different extinction ratio. In both cases, an arbitrary waveform generator (AWG) is used to generate two synchronous electric waveforms of rectangular pulse and sawtooth. The period of the sawtooth is equal to the width of the rectangular pulse. In the original scheme [see Fig. 1(a)] [8], the sawtooth is connected with a voltage controlled oscillator (VCO) that drives a single sideband modulator (SSBM) to generate an LFM continuous light; the electric pulse is launched to a Mach–Zehnder modulator (MZM) so as to achieve an optical LFM pulse with finite (typically,

* Corresponding author at: State Key Laboratory of Advanced Optical Communication Systems and Networks, Department of Electronic Engineering, Shanghai Jiao Tong University, Shanghai 200240, China.
E-mail address: wzou@sjtu.edu.cn (W. Zou).

http://dx.doi.org/10.1016/j.optcom.2016.01.034
0030-4018/

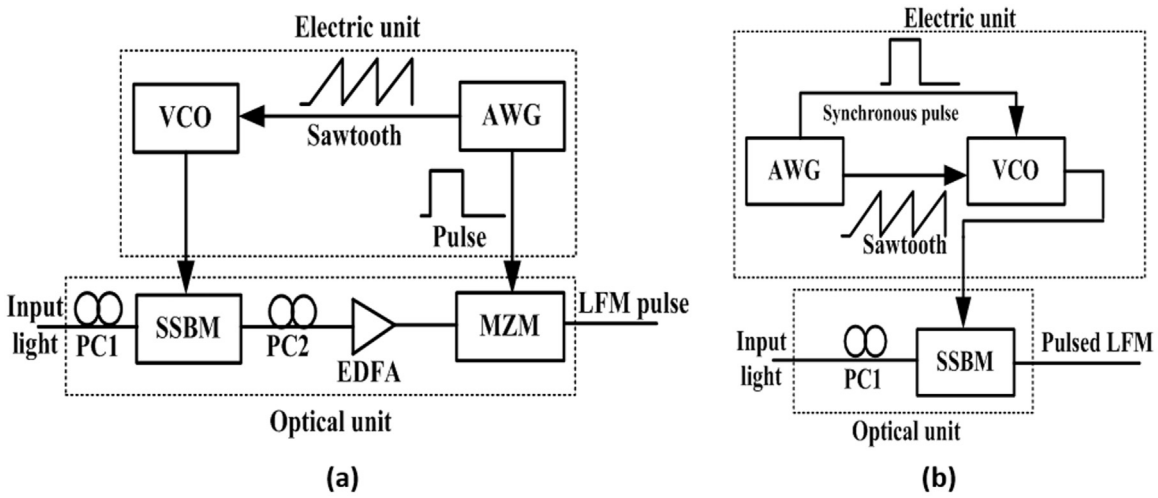

Fig. 1. Comparison of two different schemes to generate an optical LFM pulse. (a) The original scheme [8] and (b) the new scheme proposed in this work. VCO: voltage controlled oscillator; AWG: arbitrary waveform generator; SSBM: single-sideband modulator; MZM: Mach–Zehnder modulator; EDFA: erbium-doped fiber amplifier; PCs: polarization controllers.

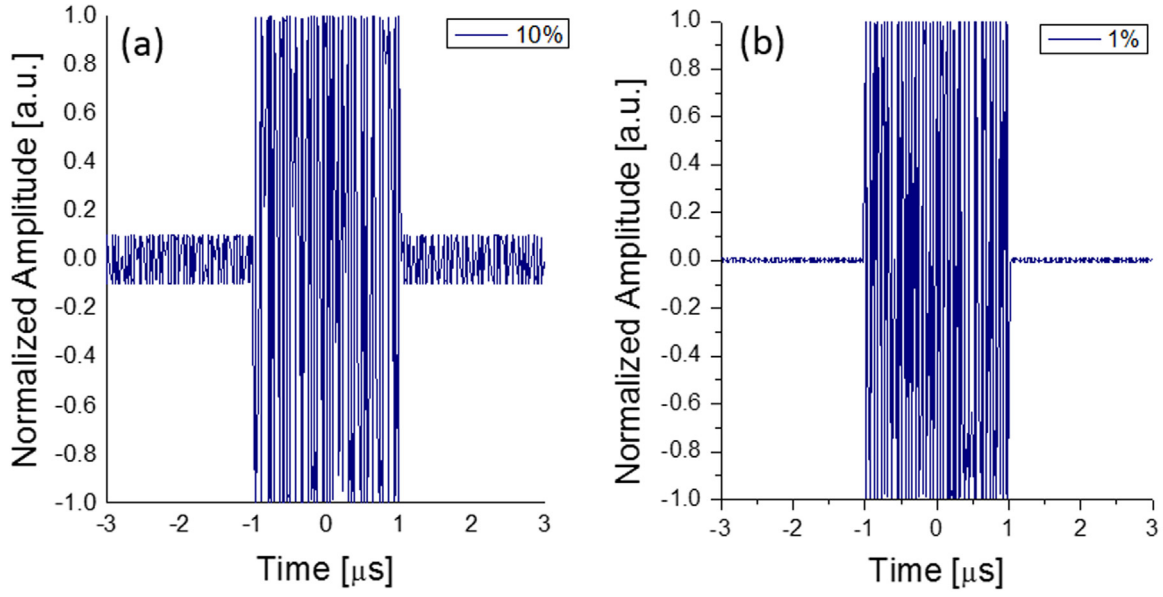

Fig. 2. Schematic comparison of the LFM pulse with different power extinction ratio. (a) $\eta=0.1$ and (b) $\eta=0.01$.

~20 dB) and unstable extinction ratio. As shown in Fig. 1(b), both electric waveforms in the new scheme are connected simultaneously with the VCO so as to generate an electrically pulsed LFM. The VCO drives the SSBM to generate an optical LFM pulse. As long as the rectangular pulse served as supply voltage switches from high-level voltage to zero voltage, the VCO changes from normal status (high voltage, V_1) to shut-down status (almost zero voltage, V_0), generating an electrically pulsed LFM with high extinction ratio. Correspondingly, an optical LFM pulse is formed with greater extinction ratio than that under the additional assistance of the MZM. Besides, the complexity of the new scheme is significantly reduced. In the new scheme, only one SSBM and one polarization controller (PC) are sufficient to generate the optical LMF pulse. However, in [8], except for this, one more MZM, PC, and erbium-doped fiber amplifier (EDFA) are required.

The electric field of SSBM is given by [10]

$$E(t) \propto J_0(m)e^{i\omega_0 t} + J_1(m)e^{i(\omega_0-\omega_{RF})t}, \tag{1}$$

where m is the modulation depth that is proportional to the driven voltage (i.e. V_{VCO}), ω_0 is the optical angular frequency, ω_{RF} is the electric angular frequency, and $J_{0,1}(m)$ denotes the Bessel functions corresponding to the magnitudes of optical carrier and single sideband. The extinction ratio of the SSBM is determined by

$$ER_{SSB} \equiv 10^* \log 10\frac{J_1(m_1)^2}{J_1(m_0)^2} \approx ER_{VCO}, \tag{2}$$

where m_1 (m_0) corresponds to the modulation depth when the VCO is high (lower) voltage of V_1 (V_0), $ER_{VCO}=20\log(V_1/V_0)$ denotes the power extinction ratio of the VCO, and the approximation is valid for low-depth modulation (the case in this study).

The backscattered curve in the OPCR is expressed by [8]

$$y(t) = A(t)*C(t), \tag{3}$$

where $A(t)$ determines the backscattered light attributed to Rayleigh scatter occurring anywhere in the fiber, splicing loss at particular points, and end reflection due to Fresnel reflection. $C(t)$ stands for the impulse response (i.e. pulse compression) of the electrically pulsed LFM given by

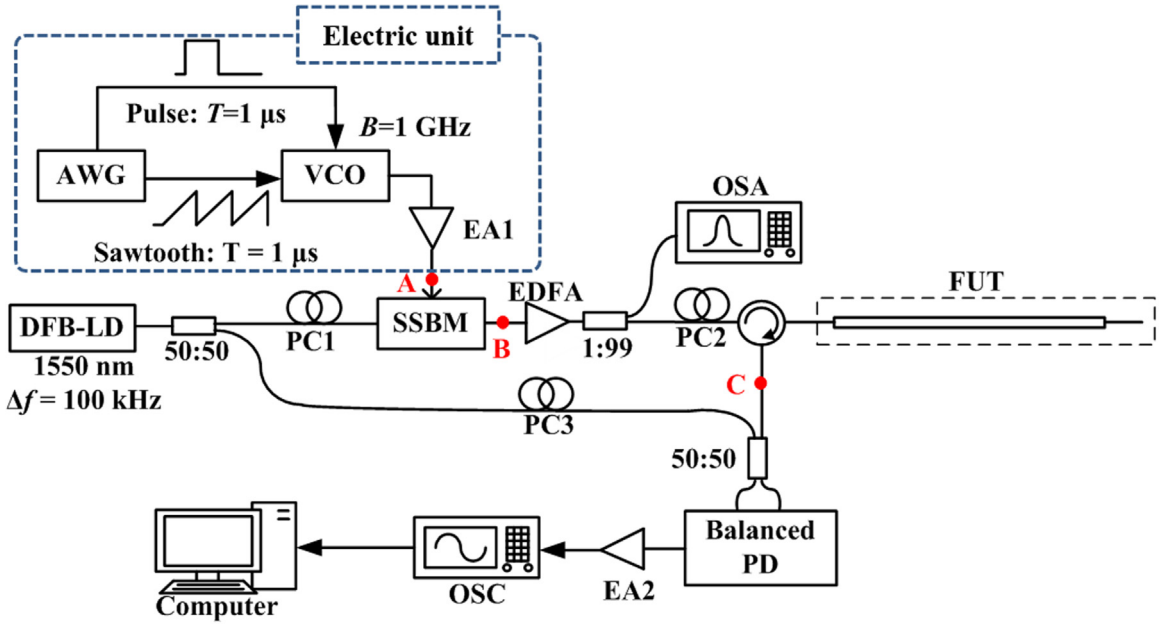

Fig. 3. Experimental setup of the modified OPCR. DFB-LD: distributed feedback laser diode; AWG: arbitrary waveform generator; VCO: voltage controlled oscillator; SSBM: single-sideband modulator; EDFA: erbium-doped fiber amplifier; EAs: electric amplifiers; OSA: optical spectrum analyzer; OSC: real-time oscilloscope; PD: photo-diode; FUT: fiber under test; PC: polarization controller.

$$C(t) = \left[\mathrm{rect}\left(\frac{t}{2T}\right) + \eta\right] \cdot T \cdot \frac{\sin[\pi K(T - |t|)(t)]}{\pi K T(t)}, \tag{4}$$

where K is the slope of the LFM, T is the pulse width, rect(•) denotes the rectangular function, $B=KT$ is the LFM sweeping range, and $\eta = V_0/V_1$ is related to the reciprocal of the ER_{SSB} as follows: $ER_{SSB} = -20\log(\eta)$. For example, $\eta=0.01$ means $ER_{SSB}=40$ dB. Fig. 2 compares the schematic of the LFM pulse with $\eta=0.1$ or 0.01, corresponding to the power extinction ratio of 20 dB [8] or 40 dB (approximately this scheme).

The spatial resolution of the OPCR is decided by [8]

$$\Delta z = \frac{c}{2nB}, \tag{5}$$

where c is the light speed in vacuum and n is the refractive index of the fiber under test (FUT).

The experimental setup of the modified OPCR is depicted in Fig. 3. The electric unit to generate the electric pulsed LFM comprises an AWG (Agilent 81150A), a VCO (Mini-Circuits ZX95-5400+), and an electric amplifier (EA1, Mini-Circuits ZX60-542LN+). A 1550 nm distributed feedback laser diode (DFB-LD, NEL NLK1C6DAAA) with a linewidth of $\Delta f = \sim 100$ kHz and a power of ~10 dBm is split into two equal beams. One beam is launched into an SSBM (Photline MXIQ-LN-40) driven by the electric pulsed LFM.

3. Results and discussion

Fig. 4(a) demonstrates the measured electric spectrum at the port of "A" in Fig. 3, providing the LFM scanned from ~4.4 GHz to ~5.4 GHz (i.e. $B = \sim 1$ GHz). Fig. 4(b) illustrates the measured time-domain profile with regular amplitude and $T=1$ μs. As shown in the optical spectrum (see Fig. 4(c)) measured by an optical spectrum analyzer (OSA) that is laid after an EDFA, a proper bias control of SSBM results in a single sideband generation with more than 15 dB suppression of the other sideband and 20 dB suppression of the optical carrier. Its frequency difference from the optical carrier is equal to the LFM. The ports of "B" and "C" in Fig. 3 are connected together for characterization of the time-domain profile of the optical LFM pulse by heterodyne detection as explained below. First, the optical beating between the local optical oscillator (i.e. the other beam of the DFB-LD, ~7 dBm) and the optical LFM pulse at a 50:50 coupler is optimized by a PC3 and detected by a balanced photo-detector (PD) with 16 GHz bandwidth (Discovery DSC720). Second, the electric signal after the balanced PD is amplified by another amplifier (EA2) and recorded by 25-GSa/s real-time oscilloscope (OSC, Tektronix DSA70804). The time-domain profile with the same $T=1$ μs is illustrated in Fig. 4(d). The power extinction ratio of $ER_{SSB}=40$ dB, corresponding to $\eta = \sim 0.01$, is deduced by the ratio of the average voltage of the pulse (i.e. the on-state of the VCO for $t \le 1$ μs) to that of the depressed component (i.e. the off-state of the VCO for $t > 1$ μs). It is noted that there is more or less amplitude varying, which is attributed to the non-uniform frequency response of the SSBM or PD and the polarization vibration of optical beating. Fig. 5 depicts the autocorrelation of the optical LFM pulse. As shown in the inset of Fig. 5, the full width at half maximum (FWHM) of ~1 ns agrees with $B=1$ GHz. Since $n=1.446$ in the single mode fiber (SMF) used in this study [9], the nominal spatial resolution is $\Delta z = 10$ cm according to Eq. (5).

First, we verify the feasibility of performance improvement of the proposed OPCR based on only one SSBM. The backscattered light of the FUT is measured by the heterodyne detection (see Fig. 3), which is the same as the characterization of the time-domain profile of the optical LFM pulse as explained in Fig. 4(d). The time-domain trace of the backscattered light recorded by the OSC is digitally I/Q converted to the complex signal. The digital matched-filtering process is implemented by use of the characterized optical LFM pulse [see Fig. 4(d)] rather than the electric LFM pulse itself [see Fig. 4(b)] that was used in [8]. For clear comparison, the preliminary measurement of the previous OPCR [8] based on two modulators with $B=200$ MHz and $T=2$ μs is plotted in Fig. 6(a). A 55-cm fiber jumper that is connected with a 5.4-km SMF spool was fairly interrogated. In contrast, a new FUT [see the inset of Fig. 6(b)] comprising the same 5.4-km SMF spool and a 15-cm fiber jumper is newly configured. As shown in Fig. 6(b), two reflection peaks of the fiber jumper at the end of the FUT are well

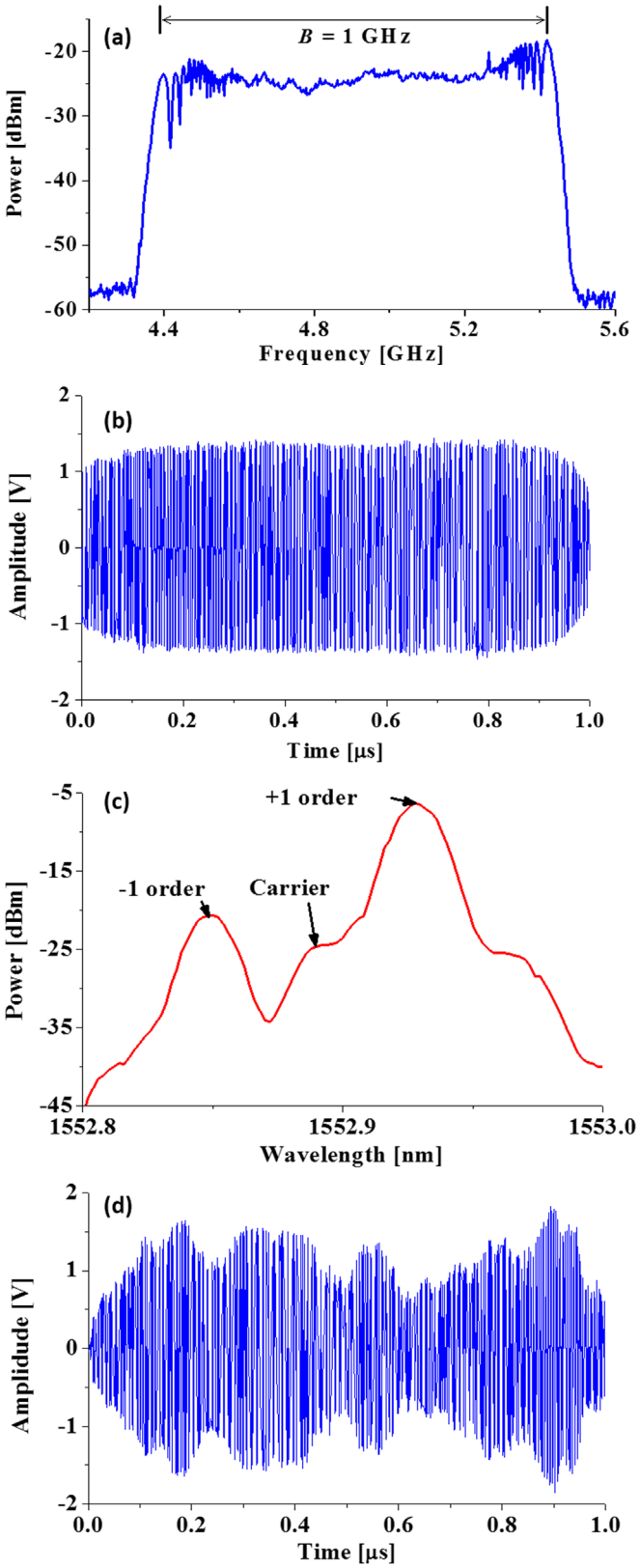

Fig. 4. Measured electric spectrum (a) and time-domain profile (b) of the electric LFM pulse. Measured optical spectrum (c) and time-domain profile (d) of the optical LFM pulse.

distinguished. Besides, the fiber loss of ~1 dB due to Rayleigh scattering is clearly recognized. Although the pulse width in this new scheme is smaller than [8], corresponding to smaller

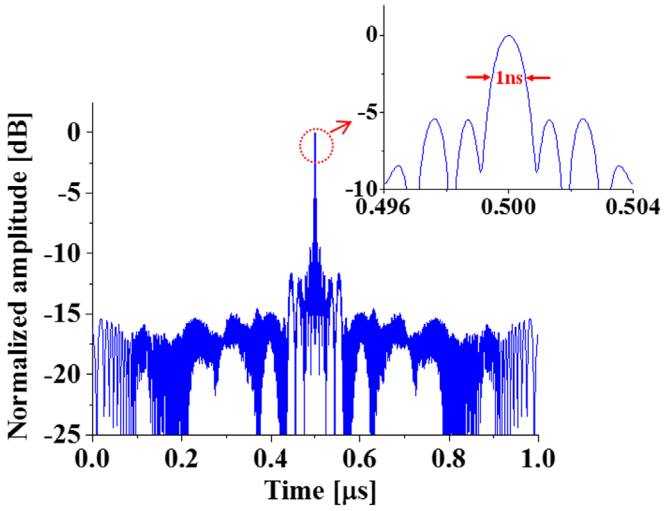

Fig. 5. Autocorrelation of the characterized optical LFM pulse. The inset denotes the magnified view around the central peak.

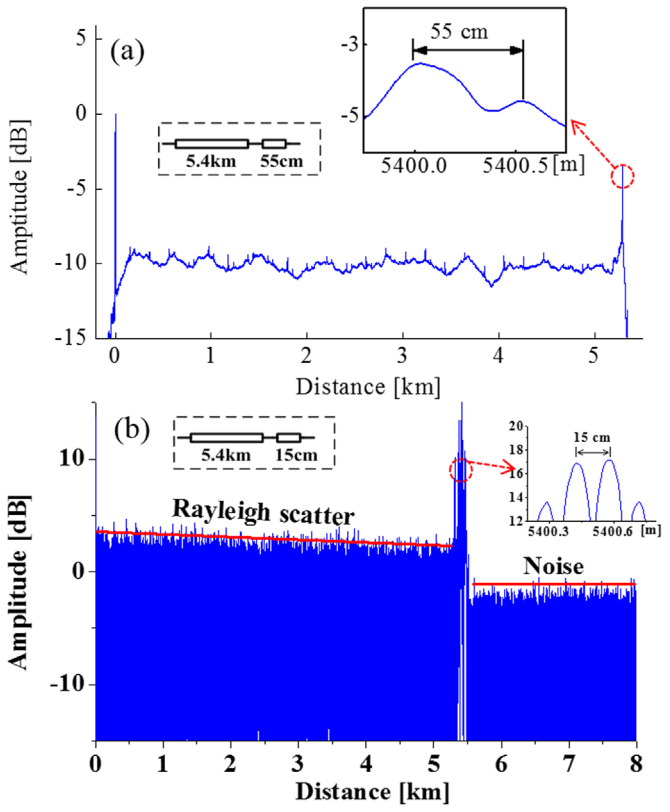

Fig. 6. Comparison of two different schemes to measure 5.4-km FUT. (a) The original scheme [8] and (b) the new scheme proposed in this work. The insets show the FUT configuration and the zoomed-in curve at the end, respectively.

signal-to-noise ratio [6], the measurement result in Fig. 6(b) is better informative than that in Fig. 6(a). The performance improvement is attributed to the increased power extinction ratio (or the reduced η) of the LFM pulse.

Fig. 7 demonstrates the numerical simulation of the back-scattering curve according to Eq. (3). The parameters of the LFM pulse are the same with the experimental ones in this study, that is, $B=1$ GHz and $T=1$ μs, except for $\eta=0.1$ or 0.01. Although strong reflections at the beginning and end of a 5.4-km FUT due to Fresnel reflections are always recognized, there are many spurious peaks existing in the curve for $\eta=0.1$, i.e. the case in [8]. This is

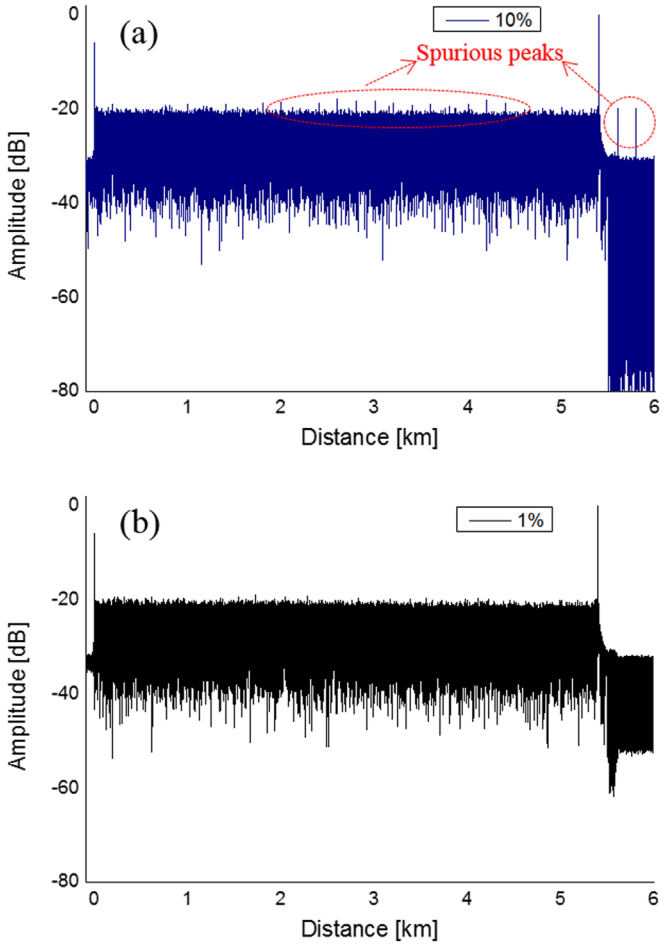

Fig. 7. Simulation comparison of two different schemes for 5.4-km FUT. (a) $\eta=0.1$ and (b) $\eta=0.01$.

physically due to the convolution of the backscattered light along the FUT and the impulse response of the LMF pulse [see Eq. (3)]. In contrast, thanks to the reduced $\eta=0.01$ of this new scheme, the backscattered light along the FUT is better localized. It is worth noting that the lower η, the better localization.

Second, we prepare another FUT by connecting two ~5.4-km SMF spools with a 15 cm jumper at the far end, as shown in Fig. 8 (a). The measured curve of the backscattered light in the FUT is illustrated in Fig. 8(b). The transmission loss of ~2 dB can be identified, which was not successfully observed in [8] due to the low power extinction ratio of the pulsed LFM. One can also see the high reflection peaks at the three different reflection points. Fig. 8 (c) shows the magnified view of these strong reflections. The two peaks due to the fiber connectors can be clearly interrogated and the FWHM of ~11 cm verifies the nominal spatial resolution of ~10 cm. There are two distinguishable peaks with an interval of 15 cm at the far end. It ensures that the measurement range is beyond ~10.8 km, which is five times larger than the coherence length of 2 km of the DFB-LD. Note that the time varying amplitude of the optical LFM pulse influences to some extent the sidelobes (see Fig. 5); besides, the sidelobes of the OPCR due to the nature of LFM pulse compression still exist in the backscattered curve [see Fig. 8(c)]. It can be possibly reduced by use of proper windowing (i.e. apodization) [6]. Besides, the measurement range may be further enlarged by an optical amplifier laid after the FUT's reflection and the circulator so as to compensate the fiber loss. These potential improvements are now under investigation.

The simulation results with the same parameters of the LMF pulse in Fig. 7 and the same FUT configuration of two cascaded 5.4-km SMF spools are depicted in Fig. 9. The advantage of this new scheme compared with [8] is similar with Fig. 7, verifying again the contribution of the reduced η to the performance (accuracy and stability) improvement.

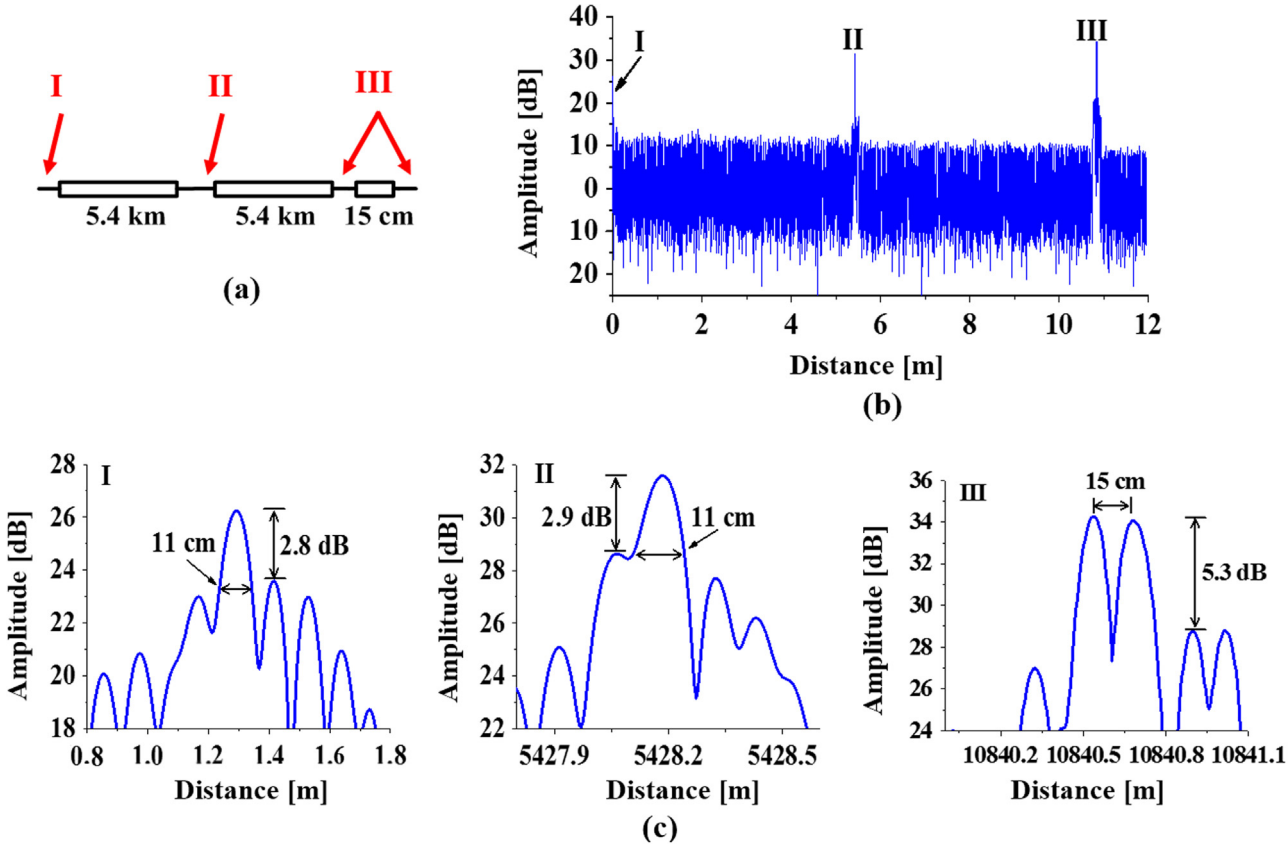

Fig. 8. (a) Configuration of the FUT with three reflection points. (b) Measured curve of backscattered light. (c) Magnified view of the (b) around three reflection points.

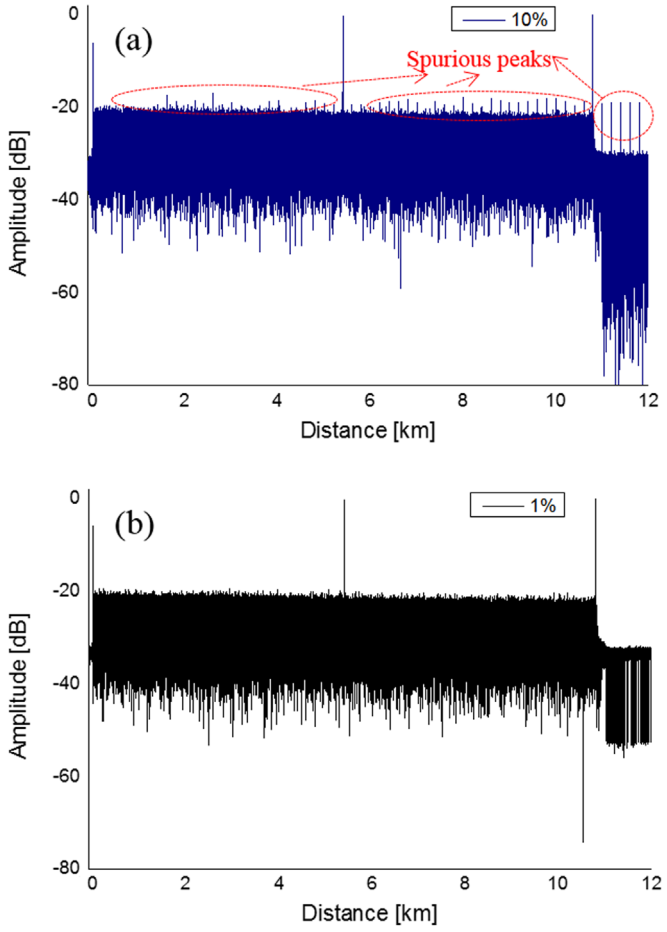

Fig. 9. Simulation comparison of two different schemes for 10.8-km FUT. (a) $\eta=0.1$ and (b) $\eta=0.01$.

4. Conclusion

We have demonstrated a modified OPCR based on the new generation of the optical LFM pulse by directly switching the VCO to generate electric pulsed LFM. The properties of the electric pulsed LFM and the optical LFM pulse are experimentally characterized. Both experimental implementation and numerical simulation verify that the modified OPCR has better performance than [8], such as less complexity, more robust stability, and better accuracy. In the experiment, high spatial resolution (10 cm) and long measurement range (10.8 km) are presented. If a technology of generating broader sweeping bandwidth by recirculating the SSBM [11] or other advanced technology [12] is adopted into the OPCR, the spatial resolution is expected to be further improved.

Acknowledgments

This work was supported in part by the National Natural Science Foundation of China under Grant 61535006 and Grant 61571292, in part by the Specialized Research Fund within the Doctoral Program through the Ministry of Education under Grant 20130073130005, in part by the State Key Laboratory Project of Shanghai Jiao Tong University under Grant 2014ZZ03016, and in part by Shanghai Key Laboratory of Specialty Fiber Optics and Optical Access Networks (Grant No. SKLSFO2015-04).

References

[1] X. Bao, L. Chen, Recent progress in distributed fiber optic sensors, Sensors 12 (2012) 8601–8639.
[2] M.K. Barnoski, M.D. Rourke, S.M. Jensen, R.T. Melville, Optical time domain reflectometer, Appl. Opt. 16 (1977) 2375–2379.
[3] B. Soller, D. Gifford, M. Wolfe, M. Froggatt, High resolution optical frequency domain reflectometry for characterization of components and assemblies, Opt. Express 13 (2005) 666–674.
[4] M. Kashiwagi, K. Hotate, Long range and high resolution reflectometry by synthesis of optical coherence function at region beyond the coherence length, IEICE Electron, IEICE Electron. Express 6 (2009) 497–503.
[5] S. Li, X. Li, W. Zou, J. Chen, Rangeability extension of fiber-optic low-coherence measurement based on cascaded multistage fiber delay line, Appl. Optics 51 (2012) 771–775.
[6] M.A Richards, Fundamentals of Radar Signal Processing, McGraw-Hill Education, United States, 2005.
[7] S. Yang, W. Zou, X. Long, J. Chen, Pulse-compression optical time domain reflectometer, in the 23rd International Conference on Optical Fiber Sensors, vol. 9157, 2014, p. 915736.
[8] W. Zou, S. Yang, X. Long, J. Chen, Optical pulse compression reflectometry: proposal and proof-of-concept experiment, Opt. Express 23 (2015) 512–522.
[9] W. Zou, Z. He, K. Hotate, Experimental study of Brillouin scattering in fluorine-doped single-mode optical fibers, Opt. Express 16 (2008) 18804–18812.
[10] K. Higuma, S. Oikawa, Y. Hashimoto, H. Nagata, M. Izutsu, X-cut lithiumniobate optical single-sideband modulator, Electron. Lett. 37 (2001) 515–516.
[11] W. Li, J. Yao, Generation of linearly chirped microwave waveform with an increased time-bandwidth product based on a tunable optoelectronic oscillator and a recirculating phase modulation loop, J. Light. Technol. 32 (2014) 3573–3579.
[12] H. Zhang, W. Zou, J. Chen, Generation of widely tunable linearly-chirped microwave waveform based on spectral filtering and unbalanced dispersion, Opt. Lett. 40 (2015) 1085–1088.